AD_____

Award Number: W81XWH-04-1-0149

TITLE: The Role of the Caspase-8 Inhibitor FLIP in Androgen-Withdrawal Induced Death of Prostate Epithelium

PRINCIPAL INVESTIGATOR: John J. Krolewski, M.D., Ph.D.
Kent Nastiuk, Ph.D.

CONTRACTING ORGANIZATION: University of California at Irvine
Irvine, California 92612

REPORT DATE: January 2005

TYPE OF REPORT: Annual

PREPARED FOR: U.S. Army Medical Research and Materiel Command
Fort Detrick, Maryland 21702-5012

REPORT DOCUMENTATION PAGE

Form Approved
OMB No. 074-0188

1. AGENCY USE ONLY (Leave blank)	2. REPORT DATE	3. REPORT TYPE AND DATES COVERED
	January 2005	Annual (1 Jan 2004 - 31 Dec 2004)

4. TITLE AND SUBTITLE
The Role of the Caspase-8 Inhibitor FLIP in Androgen-Withdrawal Induced Death of Prostate Epithelium

5. FUNDING NUMBERS
W81XWH-04-1-0149

6. AUTHOR(S)
John J. Krolewski, M.D., Ph.D.
Kent Nastiuk, Ph.D.

7. PERFORMING ORGANIZATION NAME(S) AND ADDRESS(ES)
University of California at Irvine
Irvine, California 92612

E-Mail: jkrolews@uci.edu

8. PERFORMING ORGANIZATION REPORT NUMBER

9. SPONSORING / MONITORING AGENCY NAME(S) AND ADDRESS(ES)
U.S. Army Medical Research and Materiel Command
Fort Detrick, Maryland 21702-5012

10. SPONSORING / MONITORING AGENCY REPORT NUMBER

11. SUPPLEMENTARY NOTES

12a. DISTRIBUTION / AVAILABILITY STATEMENT
Approved for Public Release; Distribution Unlimited

12b. DISTRIBUTION CODE

13. ABSTRACT (Maximum 200 Words)

Secretory prostatic epithelial cells undergo apoptosis in response to androgen deprivation. Similarly, metastatic prostate cancers, which resemble secretory epithelium, also undergo apoptosis following androgen deprivation. Recent evidence suggests that death receptor signaling is required for prostate epithelial cell death following androgen withdrawal. We sought to extend this observation by investigating the role of death receptor signaling components in models of prostate epithelial cell death. Preliminary experiments suggest that FLIP can inhibit apoptosis of prostate epithelial cells. FLIP is an enzymatically inactive version of pro-caspase-8 which negatively regulates cell death, apparently via a dominant-negative mechanism. Based on our preliminary data, we hypothesize that FLIP is a key regulator of prostate apoptosis in response to androgen withdrawal. To address our hypothesis we propose a systematic approach involving, sequentially, correlative (aim 1), functional (aim 2) and mechanistic (aims 3 and 4) experiments. The specific aims are: i) correlate the pattern of FLIP expression with prostate epithelial cell death; ii) assess the functional consequences of forced FLIP expression on prostate epithelial apoptosis; iii) determine which death receptor pathway is involved in prostate epithelial cell death and iv) determine if androgens regulate the level of FLIP expression at the level of gene transcription.

14. SUBJECT TERMS
No subject terms provided.

15. NUMBER OF PAGES
43

16. PRICE CODE

17. SECURITY CLASSIFICATION OF REPORT	18. SECURITY CLASSIFICATION OF THIS PAGE	19. SECURITY CLASSIFICATION OF ABSTRACT	20. LIMITATION OF ABSTRACT
Unclassified	Unclassified	Unclassified	Unlimited

Table of Contents

INTRODUCTION: Our long term goal is to identify the molecular events which trigger androgen withdrawal induced apoptosis (AWIA), in order to discover novel targets for prostate cancer therapy. The studies focus on FLIP, an inactive homologue of caspase-8, which inhibits apoptosis. Based on our preliminary studies, we hypothesize that FLIP plays a key role in AWIA. Specifically, we propose that FLIP protein levels are transcriptionally down-regulated following androgen withdrawal, permitting the activation of one or more death receptor signaling pathways.

PROGRESS REPORT:

Task 1. Correlate the decline in FLIP expression with the onset of prostate epithelial cell death (months 1-6).

- 1.1 Employ affinity precipitation and immunoblotting to measure FLIP protein levels in apoptosing rat prostate glands.
- 1.2 Use immunohistochemistry and *in situ* hybridization to determine the spatial (cell-type specific) pattern of FLIP expression in apoptosing rat prostate glands.
- 1.3 Measure the levels of FLIP mRNA (by quantitative RT-PCR) and protein (by affinity precipitation and immunoblotting) in NRP-152 cells induced to apoptose by TGFß.

Results: We have found that FLIP protein levels decline by 24 hours post-castration, before the onset of AWIA in the prostates of castrated rats (task 1.1). This data is shown in Fig. 1 in the Appendix. We expect that FLIP mRNA and protein levels will be mainly modulated in apoptosing secretory epithelium, rather than in apoptosis-resistant basal epithelial and stromal cells, but have not yet undertaken the studies to confirm this (task 1.2). Since differentiation sensitizes NRP-152 cells to TGFß killing, our hypothesis suggests that both FLIP mRNA and protein levels should decline in terminally differentiated NRP-152 cells. Indeed, immunoblots of NRP-152 cells undergoing differentiation show a complex regulation, with an initial decline in FLIP protein levels, followed by an increase within 24 hours. TGFß blocks this later increase in FLIP protein levels (task 1.3) (see manuscript Figs. 1 and 7).

Task 2. Assess the functional consequences of forced FLIP expression on prostate epithelial apoptosis (months 1-36).

- 2.1 Create NRP-152 cells expressing an inducible FLIP transgene and confirm our preliminary observation that FLIP overexpression inhibits TGFß induced apoptosis of this immortalized prostate epithelial cell line.
- 2.2 Generate an adenovirus expressing FLIP-IRES-GFP, infect rat prostate glands and determine if constitutive FLIP over-expression inhibits castration induced prostate epithelial cell death.
- 2.3 Create inducible FLIP transgenic mice and determine if FLIP over-expression inhibits castration induced prostate epithelial cell death.

Results: Inducible expression constructs have proven unsuitable due to the loss of TGFß responsiveness during selection of the tetracycline inducible clones. We

therefore isolated additional constitutively expressing FLIP short NRP clones to extend our analysis (see manuscript Fig 4). Forced expression of FLIP short inhibits TGFß induced cell death in NRP-152 cells and the inhibition is dependent on the level of FLIP expression. Clones expressing FLIP short fail to show the increased caspase activity that accompanies TGFß treatment of control NRP-152 cells (task 2.1) (see manuscript Figs. 1, 3 and 4). Adenoviruses expressing GFP alone and both the long and short forms of FLIP with an IRES-driven GFP cassette have been produced (data not shown). We are currently assessing whether the FLIP expressing adenovirus protects infected (green fluorescent) NRP-152 cells from TGFß induced cell death and will infect rat prostates if the are protective (task 2.2). We have not yet begun creating a mouse line with inducible expression of a FLIP transgene (task 2.3).

Task 3. *Examine the mechanism of FLIP action by determining which death receptor pathway is inhibited by FLIP during prostate epithelial apoptosis (months 24-36).*

- 3.1 Determine if Fas and/or TRAIL KO mice are resistant to, or show a reduction in the extent of, castration induced prostate cell death.
- 3.2 Determine if recombinant death receptor ligands (FasL and TRAIL) induce cell death in NRP-152 cells and primary prostate epithelial cells.

Results: Initial experiments using wild-type mice were technically unsatisfactory due to excessive variability derived from the difficulty in dissecting the prostate lobes from the surrounding tissue. We have therefore been developing an MRI method with a 7 Tesla small animal MRI since it allows us to more precisely make volume measurements of the organ and to follow the same animal over time, as it is non-invasive. Appendix Figs 2-3 summarize our findings, demonstrating the general reproducibility of the MRI measurements in assessing the size of intact prostates (Fig. 3b) and the involution of the prostate as assessed by MRI (Figs. 2 and 3A). We will then begin breeding TRAIL -/- mice in order produce mature males for assessment of the regression in these animals. We predict that TRAIL might be the death receptor ligand that mediates apoptosis in prostate epithelium and therefore, we expect TRAIL KO mice will be refractory to AWIA (task 3.1). We have demonstrated that recombinant TRAIL will induce apoptosis in NRP cells (see manuscript Fig. 6C), but while DR4-Fc and DR5-Fc block TRAIL-induced death in Jurkat cells (manuscript Figs. 6A-B), they fail to block TGFß-induced death in NRP cells (manuscript Figs. 6 D-F). We have not yet undertaken similar studies in primary prostate epithelial cells (task 3.2).

Task 4. Characterize androgen regulation of FLIP expression in the androgen-responsive cell line LNCaP.

- 4.1 Use immunoblotting, RT-PCR and reporter gene assays to determine if androgen–mediated regulation of FLIP occurs at the level of gene transcription.

Results: We have observed androgen mediated modulation of FLIP protein in LNCaP cells and predict that the FLIP gene is regulated by androgen at the level of gene transcription (Appendix Fig. 4). We have found that the regulation of FLIP is dependent on the PTEN state of the cells, and that in LNCaP cells, which lack PTEN, the PI3K inhibitor LY294002 is required to see modulation of FLIP protein (Appendix Fig. 5). We have also observed a role for Akt activators such as insulin in modulating FLIP expression (manuscript Fig. 7). We fail to find androgen regulation of several reporter constructs driven by portions of the FLIP promoter in LNCaP cells (data not shown), and are pursuing their regulation in the presence of AKT pathway modulators. We hope to define conditions where the FLIP protein and mRNA, as well as a reporter gene under the control of the FLIP promoter region, will all decline in cells grown at low androgen concentrations.

KEY RESEARCH ACCOMPLISHMENTS:

- Define the complex regulation of FLIP protein in differentiating NRP cells
- Isolate and characterize additional FLIP short expressing NRP clones
- Production of adenoviruses expressing FLIP short and long with IRES-GFP
- Developed MRI methodology to measure prostate volume changes in the same animal over time.

REPORTABLE OUTCOMES:

1. Presentation at the UCI Cancer Center retreat, 11/04
2. Presentation at the UCI Campuswide Cancer Symposium, 5/05
3. Manuscript submitted to Oncogene, 8/05
4. Production of two novel adenoviruses, rat FLIP short and long

CONCLUSIONS: We have made good progress in overcoming the inherent problems working with normal rodent prostate biology. The shifting phenotype during selection of clones of NRP cells for isolation of inducible FLIP clones made it a less desirable alternative than isolation of additional constitutively expressing clones to characterize TGFß-induce apoptosis. The small size and interdigitated nature of the mouse prostate made characterizing AWIA much less reliable than in the rat. We therefore developed the MRI method, which should be both more precise, since we will be able to sample the same animal over time, rather than the mean of groups of mice sacrificed at different times. Regulation of FLIP in the human prostate cancer cell line LNCaP has proved challenging to describe, but it appears that androgen regulation of FLIP in these cells may be affected by their lack of PTEN. We expect that prostate cells with wild-type levels of PTEN will show more consistent regulation of FLIP by androgens.

REFERENCES: None

APPENDIX: See attached

APPENDIX

FIGURE 1 FLIP protein levels decline following castration

FIGURE 2 MRI documents involution of mouse prostate following castration

FIGURE 3 Quantitation of MRI data

FIGURE 4 FLIP protein levels decline in response to increasing androgen levels in LNCaP prostate epithelial cells

FIGURE 5

MANUSCRIPT (submitted to Oncogene)

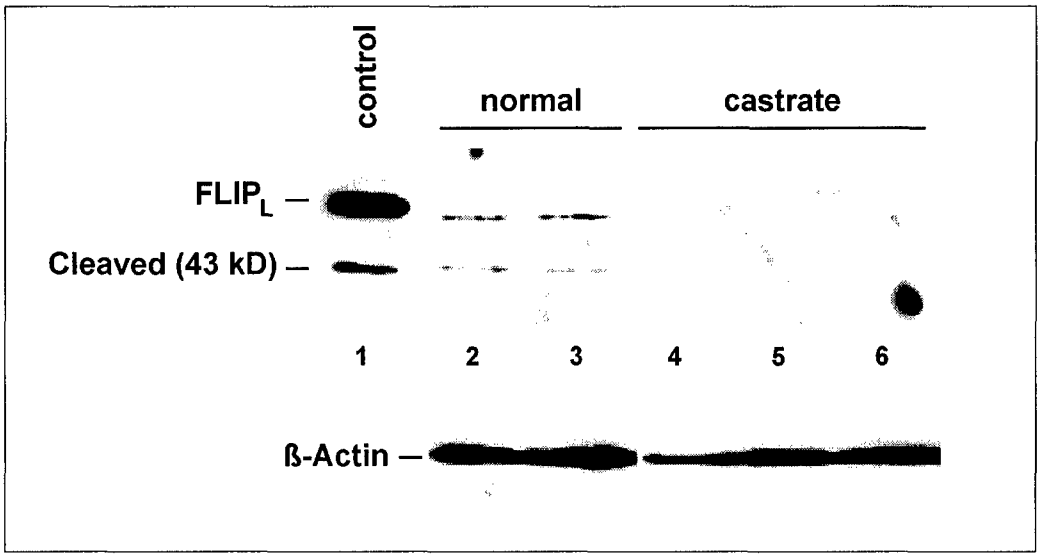

Appendix Figure 1. FLIP protein levels decline following castration. Rats were surgically castrated or sham operated and 24 h later prostate glands were removed and protein lysates prepared. MBP-DED fusion proteins were used to affinity precipitate FLIP proteins (in the presence of z-VAD to prevent caspase activation during purification) and the resulting protein complexes were immunoblotted with an anti-FLIP antibody (upper panels). Extracts were probed with anti-actin to confirm that equal amounts of protein were input to each affinity precipitation reaction. Each lane represents protein recovered from a separate animal (two sham and three castrated animals). As can be seen, the level of FLIP protein declines in the glands from castrated animals, relative to intact animals.

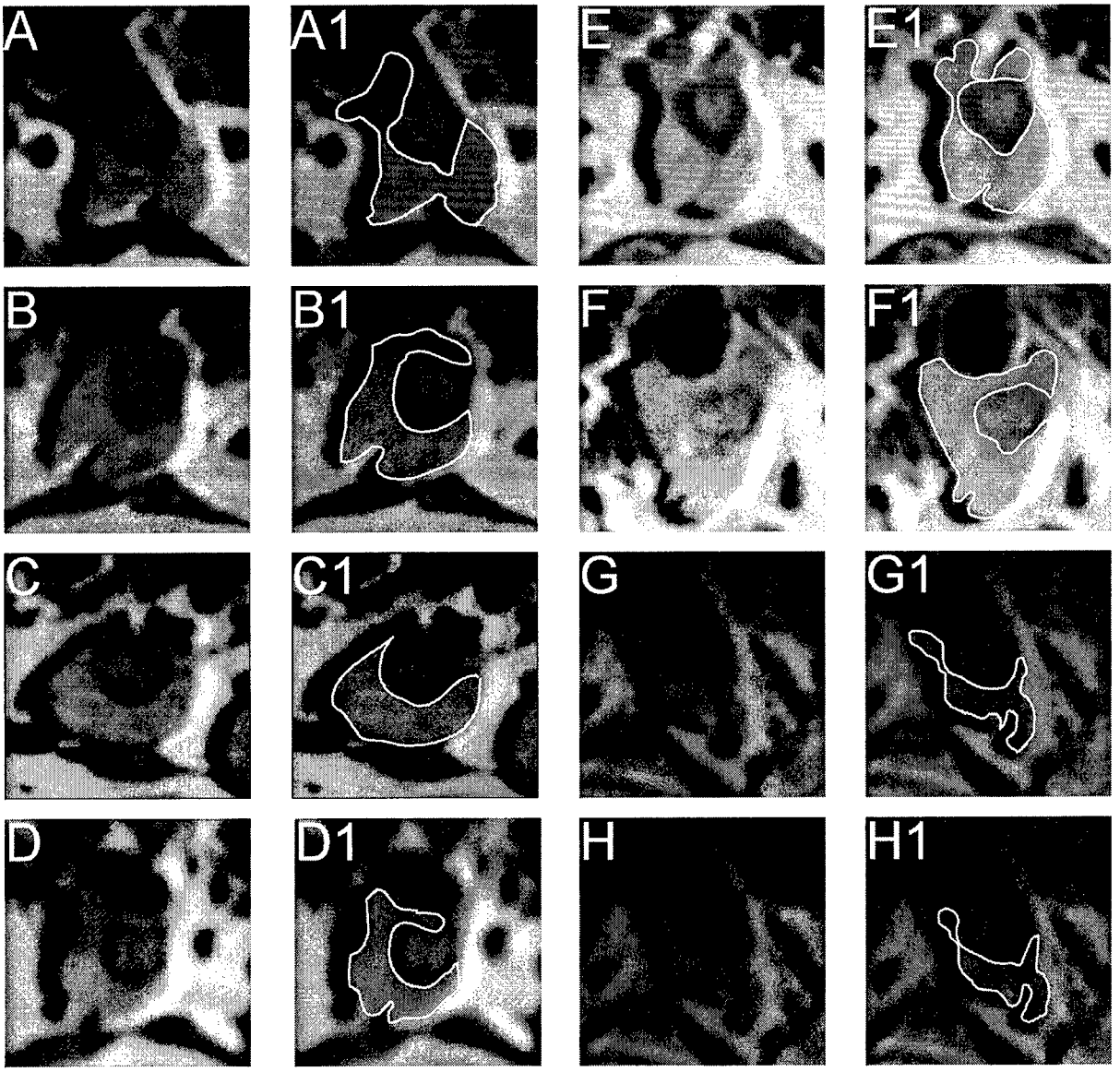

Appendix Figure 2. MRI documents involution of mouse prostate following castration. Adult male mice were either left intact (A-D) or castrated (E-H) and then subjected to imaging via MRI. Panels A-D correspond to four different normal males (A = b3m2; B = b3m3; C = b4m1; D = b2m3). The corresponding panels A1-D1, show an outline of the ventral lobe of the prostate in one MRI image level. Panels E-H correspond to a single castrated mouse which was imaged at 1, 3, 8 and 10 days post-castration, respectively. The corresponding panels E1-H1, show an outline of the ventral lobe of the prostate in one MRI image level.

A

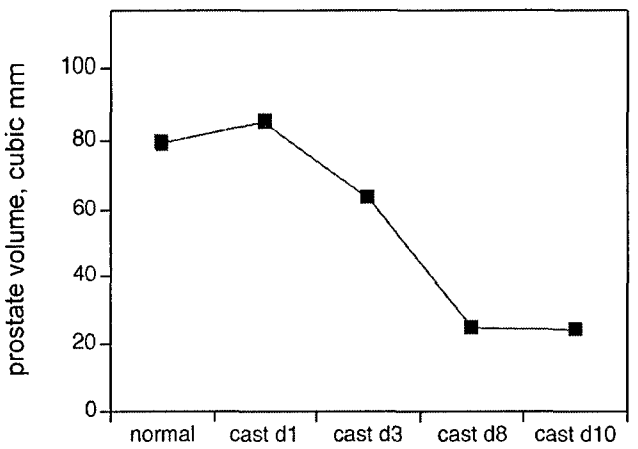

B

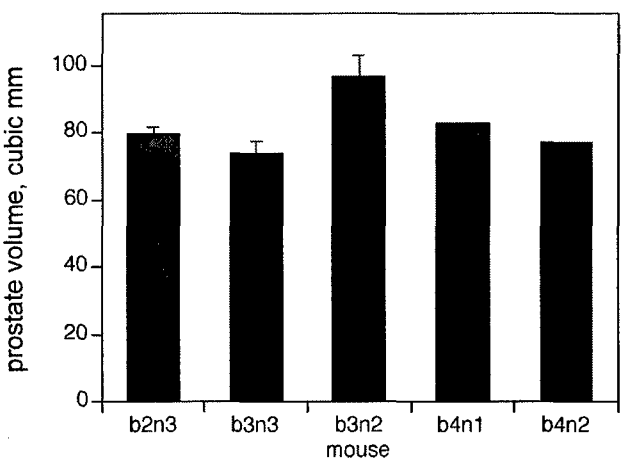

Appendix Figure 3. Quantitation of MRI data. Panel A. MRI-derived ventral prostate lobe volume declines post-castration. Prostate volumes were determined by manually encircling the ventral lobe on each MRI 'slice' and then summing the area of all such slices of the MRI images corresponding to those shown in panels E-H of Appendix Figure 2. These volumes were then plotted as a function of time. As can be seen, there is a clear reduction in the volume of the ventral lobe following castration, which resembles the kinetics of involution observed for the rat prostate (based on weight). Panel B. MRI determined prostate volumes are reproducible among a cohort of normal mice. MRI images were used to calculate ventral prostate volumes as in panel A. The mouse designations are given in Figure 2A-D. Note the good reproducibility from animal to animal.

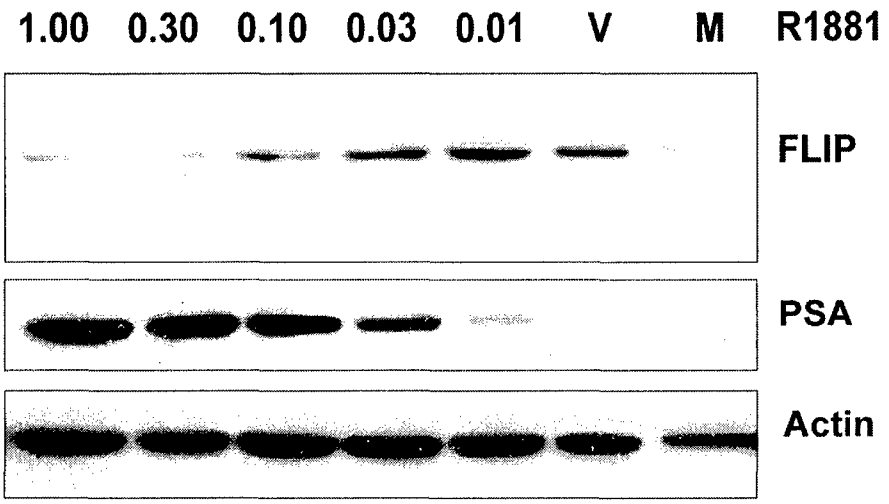

Appendix Figure 4. FLIP protein levels decline in response to increasing androgen levels in LNCaP prostate epithelial cells. LNCaP cells were grown in media with charcoal-striped serum. Varying amounts of R1881 (as indicated) were added to the cultures and 24 h later post-nuclear supernatant protein extracts were immunoblotted and probed with antibodies against FLIP, PSA and actin (loading control). Lane V corresponds to cells treated with vehicle only. PSA levels indicate the level of androgen response.

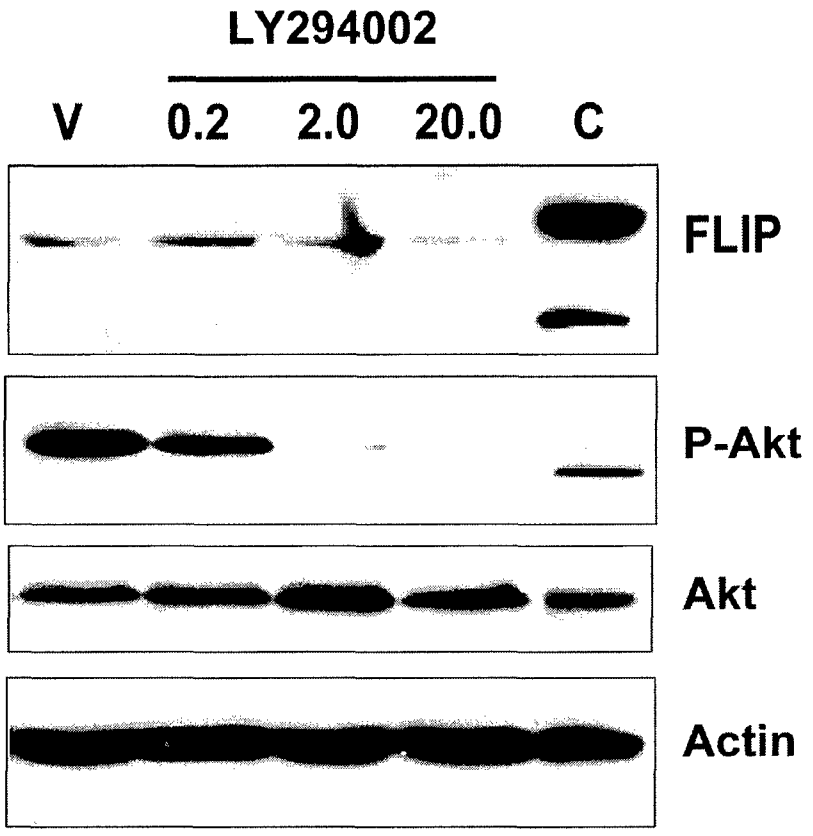

Appendix Figure 5. Inhibition of PI3K-Akt activity by LY294002 decreases FLIP protein levels. LNCaP cells were grown in media with charcoal-striped serum. Varying amounts of LY294002 were added to the cells and 24 h later post-nuclear supernatants protein lysates were prepared and immunoblotted with the indicated antibodies. LNCaP cells are deficient in PTEN and thus have a constitutively active Akt. As shown, increased levels of the inhibitor reduce the level of FLIP protein.

FLICE-like inhibitory protein blocks TGFß1 induced caspase activation and apoptosis in prostate epithelial cells

Kent L. Nastiuk[1], Karen Lo[1], Kevin Su[1], Patricia Yeung[1], Julia Kutaka[1], Andrew Cornforth[1], and John J. Krolewski[*,1,2]

[1]Department of Pathology and Laboratory Medicine,

[2]Chao Family Comprehensive Cancer Center,

University of California, IRVINE,

Irvine, CA 92697-4800, USA

***Correspondence:**

JJ Krolewski, Department of Pathology and Laboratory Medicine, College of Medicine, UC IRVINE, Medical Sciences D450, Irvine, CA 92697-4800; E-mail :jkrolews@uci.edu

Phone: 949-824-4089

Running Title: FLIP blocks apoptosis of prostate epithelial cells

Key Words: FLIP, apoptosis, TGFß, caspase, prostate epithelial cells, NRP-152

Abstract

Androgen withdrawal induces regression of human prostate cancers, but such cancers eventually become androgen independent and metastasize fatally. Thus, deciphering the mechanism of androgen-withdrawal induced apoptosis (AWIA) is critical to designing new therapies for prostate cancer. Previously, we demonstrated that in the rat, castration-induced apoptosis is accompanied by a reduction in the expression of the apical caspase inhibitor FLIP (FLICE-like inhibitory protein). To test the functional role of FLIP in inhibiting prostate epithelial cell apoptosis, we employed the rat prostate epithelial cell line NRP-152 (NRP). NRPs differentiate to a secretory phenotype in low-mitogen media and then undergo apoptosis following TGFß addition, mimicking AWIA. NRPs were stably transfected with constitutively expressed FLIP. Clones expressing higher levels of FLIP were refractory to TGFß induced apoptosis. TGFß induced caspase-3 activity is proportional to the level of cell death and FLIP expression in each clone. Neither caspase-3 nor PARP is cleaved in clones expressing high level FLIP. To assess whether a death receptor (DR) ligand is involved in TGFß induced apoptosis, we used DR-Fc chimeric proteins that block ligand-receptor interactions. Neither Fas-Fc, DR4-Fc nor DR5-Fc blocked TGFß induced cell death. However, insulin signaling inhibits NRP death, suggesting that FLIP blocks other DR-ligands and/or mitochodrial apoptosis. [201 words]

Introduction

Androgens regulate the growth of both normal and neoplastic prostate, and androgen signaling blockade is the primary treatment for late stage prostate cancer. Thus, there is an urgent need to understand the molecular events regulating androgen withdrawal-induced apoptosis (AWIA). As in humans, androgens promote mitosis and differentiation of rodent prostate ductal epithelium, and further, appear to inhibit apoptosis of differentiated cells (Isaacs, 1984). After androgen ablation, the balance between mitosis and apoptosis is disrupted, and within two days markers of apoptosis, such as fragmentation of chromosomal DNA, are evident (Colombel & Buttyan, 1995; Nastiuk, 2003). The prostate undergoes a wave of cell death resulting in the involution of the gland (Brodin et al., 1999).

A variety of evidence indicates that TGFß1 (TGFß) is a paracrine and/or autocrine mediator of AWIA in the intact animal. AWIA is accompanied by an increase in TGFß1 mRNA, and the kinetics of mRNA induction closely parallel those of AWIA (Kyprianou & Isaacs, 1989). Additionally, there is a concomitant rise in the expression of the RI and RII subunits of the TGFß receptor(Kim et al., 1996) as well as phosphorylated Smad2, a key downstream mediator of TGFß (Brodin et al., 1999). A dominant negative form of TGFß-RII blocks TGFß induced differentiation and cell death (Kundu et al., 2000; Tang et al., 1999). Finally, administration of TGFß to non-castrated rats results in apoptosis of the prostate (Kyprianou & Isaacs, 1989; Martikainen et al., 1990). Although the mechanism of TGFß action is unclear (it might involve transcriptional effects on pro- and anti-apoptotic proteins (Coyle et al., 2003)), one potential downstream target is the family of death receptor (DR) signaling ligands.

We have previously shown that one inhibitor of the DR pathways, FLICE-like inhibitory protein (FLIP), is down-regulated in advance of AWIA in the rat prostate (Nastiuk, 2003). FLIP is an inactive homologue of caspase-8, an apical caspase activated in DR signaling. Like caspase-8, FLIP can be recruited to the DR complex following ligand binding, via the adaptor molecule FADD. Elevated levels of FLIP can displace caspase-8 from the activated DR complex, acting as a dominant inhibitor of caspase-8 and thereby preventing the activation of distal caspases and cell death (Peter & Krammer, 2003). Four extracellular ligands of the TNF family initiate apoptosis through the DRs: TNFa, TRAIL, TWEAK, and FasL. The best characterized of these DR ligands is FasL, which signals through the Fas receptor to initiate a cascade of proximal and then distal caspase activation, release of the mitochondrial contents and further caspase activation. This leads to fragmentation of chromosomal DNA, various proteins, and cellular membranes, resulting in cell death (Nagata, 1997)(Nagata & Golstein, 1995). Surgical specimens from normal human prostate, as well as both androgen responsive and unresponsive tumors, express Fas and FasL (Sasaki et al., 1998)(Xerri et al., 1997). TRAIL induced apoptosis can be inhibited by FLIP (Bin et al., 2002)(MacFarlane, 2003). TRAIL also induces apoptosis of both normal prostate epithelial cells (Nesterov et al., 2002) and prostate cancer cell lines (Yu et al., 2000)(Voelkel-Johnson et al., 2002) but many TRAIL resistant cancers are resistant to TRIAL-induced apoptosis due to overexpression of FLIP. This resistance can be overcome by blocking FLIP expression using chemotherapeutics (Kelly et al., 2002) or siRNA (Siegmund et al., 2002)(Zhang et al., 2004)(Rippo et al., 2004)(Abedini et al., 2004).

To test the functional role of FLIP in inhibiting prostate epithelial cell apoptosis, we employed the immortalized, non-tumorigenic rat prostate epithelial cell line NRP-152 (NRP) (Danielpour et al., 1994). When grown in mitogen-rich media these cells resemble prostate basal

epithelia and divide rapidly. In mitogen-poor media, growth slows and the cells differentiate into a secretory phenotype (Danielpour, 1999). The ability of NRP cells to replicate as basal-like epithelial cells and subsequently differentiate into secretory-like epithelial cells *in vivo* and *in vitro* suggests this cell line is an excellent model for prostatic epithelium. It is the secretory epithelium of the prostate which apoptoses after androgen withdrawal. Importantly, the physiologic process of AWIA can be mimicked in NRP cells *in vitro*, by the addition of TGFß1 to cultures previously differentiated in mitogen-poor media. NRPs maintained in mitogen-rich media are resistant to TGFß induced apoptosis (Hsing et al., 1996). This appears to be due to activation of the Akt/mTOR pathway, which suppresses Smad3 activation (Song et al., 2003). Our previous observation that castration-induced down-regulation of FLIP in the rat prostate immediately precedes the onset of apoptosis, suggested that FLIP might have a functional role in regulating the apoptosis of prostate epithelium that occurs following androgen withdrawal. The current report tests this possibility, employing TGFß induced apoptosis of NRP cells as a model for AWIA in the rat prostate.

Results

NRP-152 cells grown in rich media (GM2), then re-plated in low growth factor media (GM3), rapidly differentiate to a luminal (secretory) prostatic phenotype, both morphologically and biochemically (Danielpour, 1999). The proliferation of these cells slows markedly from a doubling time of less than a day to more than three days (Figure 1a, cross-hatched bars and data not shown (DNS)) but they do not apoptose (Figure 1a, squares). If, after 3 h in differentiation media, the cells are treated with 5 ng TGFß1/mL, the adherent live cells decline by about half at

two days while the apoptotic cells increase ten-fold relative to the untreated controls (Figure 1A, black bars and circles). Nucleosomal cleavage of DNA isolated after TGFß1 treatment shows that the apoptosis is evident as early as 10 h after TGFß1 addition (Figure 1b). Within 6 h, the activity of caspase-3 in TGFß1 treated cells is elevated relative to untreated NRP-152 cells. Caspase-3 activity continues to rise through 36 h TGFß1 treatment (Figure 1c). Immunoblots of nuclear extracts of NRP cells either untreated or treated with TGFß1 for up to 72 h (Figure 1d), show that one substrate of caspase-3, poly(ADP-ribose)polymerase (PARP), is also cleaved in the TGFß1 treated cells with a maximum at 36 h treatment. The initial high level of PARP cleavage at 12 h is likely due to TGFß1 effects on cells that fail to differentiate and die as a result of the low level of growth factors in the differentiation media. Since we have previously shown FLIP is reduced during rat prostate apoptosis, cytoplasmic protein isolated from a combination of adherent and floating cells at each timepoint was examined by immunoblotting for FLIP. Figure 1e shows that FLIP protein is low when the NRP cells are re-plated in differentiation media and subsequently show increasing amounts of FLIP 24-60 h after differentiation. Differentiating NRP cells treated with TGFß1, in contrast, express low FLIP levels for up to 48 h following treatment.

The decline in FLIP levels in response to TGFß1 may leave NRP cells more vulnerable to apoptosis. To test this hypothesis, we transfected a constitutively expressed FLIP gene into NRP cells and selected clonal lines expressing low or high levels of FLIP. FLIP is expressed in two isoforms: FLIP long ($FLIP_L$) which has two DED domains at the amino-terminus, followed by a caspase domain containing inactivating mutations, and FLIP short ($FLIP_S$), which contains only the two DED domains. High level over-expression of $FLIP_L$ has been previously reported to induce apoptosis via a mechanism that is poorly understood (Goltsev et al., 1997; Inohara et al.,

1997; Shu et al., 1997). Therefore, we transfected NRPs with either an HA-tagged $FLIP_S$ construct, or the corresponding empty vector, and isolated clonal lines. To assess apoptotic response, cells were differentiated in GM3 and treated with TGFß1. Differentiated parental NRP cultures treated with TGFß1 contain more than three times as many apoptotic cells as untreated differentiated cultures (Figure 2a, bar labeled P). Cultures from clones transfected with vector alone display somewhat less apoptotic response to TGFß1 (Figure 2a, V1; Figure 4a, V2 and DNS). This may be due to extended passaging during the selection process, which can produce clones partially resistant to TGFß1 (Hsing et al., 1996). Of forty-eight G418-resistant clones screened for $FLIP_S$ one showed high, and two others very low, levels of anti-HA immuno-reactivity (Figure 2b and DNS). When the resistant but non-expressing clones were assessed for TGFß1 induced apoptosis, a range from 150-350% (relative to the untreated, differentiated control) was seen (Figure 2a). The two low expressing clones (14 and 42) had 250% of untreated apoptosis, while the one clone (12) expressing a high level of $FLIP_S$ showed no increase in TGFß1 induced apoptosis (Figure 2a). Similarly, when DNA was isolated from these clones 72 h after TGFß1 treatment, internucleosomal cleavage is evident in samples from parental (P), vector-transfected (V), low expressing (14, 42) and non-expressing (32, 37) clones, but there is no cleavage of the DNA isolated from the clone (12) expressing high levels of $FLIP_S$ (Figure 2c).

Cytosolic extracts were prepared from differentiated clones and caspase-3 enzymatic activity was determined (Figure 3b). The induction of caspase activity in TGFß1 treated versus untreated cells ranged from five to fifteen fold in parental (P), vector only (V1), and low expressing clones (32, 37). The clone (12) expressing high levels of $FLIP_S$ showed no induction of caspase-3 activity (Figure 3b). The level of induction of caspase-3 activity correlated closely

with the level of TGFß1 induced apoptosis (compare Figures 3a and 3b). The extracts used in Figure 3b were separated by SDS-PAGE and immunoblotted using an antibody that detects both full-length caspase-3 (32 kD) and its active fragment (17 kD). The top panel of Figure 3c shows that TGFß1 treated and untreated extracts have approximately equal amounts of caspase-3, but a long exposure of the lower portion of the blot shows that the 17kD fragment is induced in extracts from all of the TGFß1 treated clones except clone 12 (Figure 3c, lower panel). Similarly, the caspase-3 substrate PARP is cleaved from 117 kD to an 84 kD fragment after TGFß1 treatment in all clones except clone 12 (Figure 3d).

There is a strong correlation between $FLIP_S$ expression, caspase-3 activity and apoptosis for this set of clones, but the variability in TGFß1 response after selection and the lack of response in the low expressing clones suggested that analysis of an additional set of $FLIP_S$ expressing clones might be informative. We therefore isolated an additional set of clones. Two of 48 G418 resistant clones in this second set expressed relatively high levels of $FLIP_S$ (Figure 4b, top panel) with clone 66 expressing several times more $FLIP_S$ than clone 48. Extended exposure of the immunoblot reveals that three additional clones display low level expression (Figure 4b, second panel). Each of these low expressing clones has similar levels of endogenous $FLIP_L$ when normalized to actin (Figure 4b, third and fourth panels). The level of transgenic $FLIP_S$ expression in clones 48 and 66 is roughly equivalent to the level of endogenous $FLIP_L$ in each of the clones (Figure 4b, third panel and DNS), while the three low expressing clones (61, 43, 53) have significantly less short than long. Apoptosis in response to TGFß1 ranged from 280-375% for the vector clones (Figure 4a, V2 and DNS) and non-expressing clones (44, 51 in Figure 4a and DNS). The three low expressing clones had an intermediate level of apoptosis (140-180%) while the clone with a higher level of $FLIP_S$ expression (48) had 130%, and the

highest expressor (66) only 80%, of the TGFß1 induced apoptosis relative to untreated controls (Figure 4a). Again, caspase-3 activity was highly induced (~15-fold) after TGFß1 treatment of the vector containing and $FLIP_S$ non-expressing clones (Figure 4c). The low expressing clones had a highly attenuated induction (~2-fold), while the two high expressors showed no induction of caspase-3 activity (Figure 4c). Induction of PARP cleavage was only seen in the vector containing and the non-expressing clones (V2, 44, 51 in Figure 4d) while there was no TGFß1 induced cleavage in any of the $FLIP_S$ expressing clones. Thus, Figures 2-4 indicate that forced over-expression of $FLIP_S$ protects NRP cells from TGFß1 induced caspase activation and cell death.

FLIP is thought to block DR induced activation of the apical caspases -8 and -10. Since the Fas DR has been implicated in prostate apoptosis (Hedlund et al., 1998; Hedlund et al., 1999; Rokhlin et al., 1997), we sought to determine if TGFß induced apoptosis requires Fas signaling, by employing Fas-Fc to block the FasL-Fas interaction. Initial experiments using human Fas-Fc did not block cell death (DNS). Since rat Fas differs from human Fas, a chimera (rFas-Fc) containing a CD5 leader, the extracellular domain of rat Fas fused to Fc and a carboxy-terminal HA tag was expressed in 293T cells and purified on a protein A column (Figure 5a). Jurkat cells were then used to validate the molecular reagents (Figure 5b). Specifically, treatment with 200 pg/ml of membrane bound FasL (mFasL) induced cell death after 18 h (diagonal striped bars). Further addition of Fc had no effect, while rFas-Fc completely blocked mFasL mediated killing. If TGFß1 induced apoptosis is mediated via the FasL-Fas pathway, the kinetics of death should be similar for mFasL and TGFß1. Indeed, when NRP cells are treated with mFasL, there is very little cell death apparent until 48 h and it is maximal at 72 h (Figure 5c and DNS). In addition, NRP cells are less sensitive than Jurkat cells to mFasL, with a ten-fold higher dose (2 ng/ml)

required for complete NRP killing (DNS). The addition of rFas-Fc blocks mFasL induced killing (Figure 5c, compare black and horizontally striped bars), but does not effect killing at two doses of TGFß1 (1 ng/ml, diagonally striped bars; 5 ng/ml, checkered bars). Similarly, neither 5- nor 25-fold increases in the amount of rFas-Fc significantly reduced the apoptosis induced by 1 ng/ml TGFß1 in these cells (Figure 5d).

Since rFas-Fc was unable to block TGFß1 apoptosis, we examined another death receptor pathway that might be blocked by FLIP. Specifically, since TRAIL kills neoplastic and normal human prostate epithelial cells (Nesterov et al., 2002) via activation of the apical caspases (Rokhlin et al., 2002), we examined its role in TGFß1 mediated apoptosis. TRAIL can bind two different receptors, DR4 and DR5, and Fc fusions of the extracellular domains of these receptors block TRAIL-induced cell death (Nesterov et al., 2002). As in Figure 5, we employed Jurkat cells to demonstrate the utility of DR4-Fc and DR5-Fc. Although treatment with DR4-Fc alone was partially toxic to Jurkat cells, DR4-Fc was able to block TRAIL induced death, particularly at lower concentrations of TRAIL (Figure 6a). DR5-Fc was also able to block TRAIL induced cell death (Figure 6b). TRAIL killed NRP cells but, as was the case for mFasL, only at significantly higher concentrations relative to the dose that was effective in killing Jurkat cells (Figure 6c). Since DR4-Fc and DR5-Fc were most effective blocking lower TRAIL doses, we treated NRP cells with varying doses of TGFß1, from 0.1 ng/ml, which is sub-lethal, up to 5 ng/ml and found the minimum concentration necessary to induce apoptosis is 0.5 ng/ml (Figure 6d-e, solid bars). As was the case for the Jurkat cells, DR4-Fc treatment of NRP cells was partially toxic in the absence of TGFß1 (Figure 6d, bars at far left). However, neither DR4-Fc nor DR5-Fc inhibited TGFß1 induced apoptosis of NRP cells (Figure 6d-e, solid vs striped bars). Since the two TRAIL receptors might have complementary roles in signaling (Leverkus et al.,

2003), we also employed DR4-Fc and DR5-Fc in combination, but again observed no effect on TGFß1-induced cell death (Figure 6f).

Finally, we sought to determine if growth factors that modulate the growth and differentiation of NRP cells also regulate FLIP expression. Insulin and epidermal growth factor (EGF) both stimulate NRP proliferation in the presence of 10% fetal bovine serum (Danielpour et al., 1994), but only insulin (as well as the related growth factor IGF-1) inhibits the differentiation of NRP cells from the basal to the luminal phenotype (Danielpour, 1999). Insulin addition to the cell medium during differentiation effectively blocks TGFß1 induced apoptosis as reported previously by others (Hsing et al., 1996; Song et al., 2003), while EGF addition does not (Figure 7a, striped bars). Both insulin and EGF induce an increase in the level of $FLIP_L$ in differentiating cells, but the kinetics are distinct. Specifically, when NRP cells are differentiated in the presence of insulin, $FLIP_L$ protein levels increase significantly after 6 h (Figure 7b, lanes 3-4) and remain elevated at 24 h and 48 h (Figure 7c, lanes 2 and 6). In contrast, when EGF is added to differentiating NRP cultures, $FLIP_L$ levels rise only slightly after 6 h (Figure 7b, lanes 1-2) before increasing significantly at 24 h and 48 h (Figure 7d, lanes 2 and 6). Figure 1 demonstrated that treatment of differentiated NRP cells with TGFß1 down-regulates $FLIP_L$ protein levels and coordinately induces apoptosis. Similarly, Figure 7c-d (lanes 3-4 and 7-8) shows that TGFß1 reduces $FLIP_L$ expression and induces PARP cleavage, a marker of apoptotic caspase activation. Insulin prevents the TGFß1 induced reduction of $FLIP_L$ at both 24 h (Figure 7c, lanes 1 and 3) and 48 h (Figure 7c, lanes 5 and 7) and effectively prevents PARP cleavage. EGF is not effective at reducing $FLIP_L$ expression and only partly effective at inhibiting PARP cleavage (Figure 7c, lanes 1,3, 5 and 7). Thus, treatment of differentiated NRP cells with with these two growth factors further demonstrates that TGFß1 induced apoptosis is inversely

correlated with the level of $FLIP_L$ expression.

Discussion

Normal prostate cells secrete TGFß when induced to apoptose via androgen ablation. The NRP cell line does not apoptose in our hands when androgen is withdrawn from the culture media, but do when treated with TGFß. Caspases are activated, the DNA fragments, and the cell number declines (Figure 1). Since we see modulation of the FLIP mRNA transcript and protein levels in castrated rats (Nastiuk, '03), we sought to determine whether continuous expression of FLIP in the presence of an apoptosis inducer in normal rat prostate cells would be sufficient to block apoptosis in NRP cells. We chose to express FLIP short since FLIP long over-expression spontaneously induces cell death. While we do not necessarily believe that FLIP short is the relevant FLIP isoform in NRP cells (indeed we have not detected it in NRP cells) we were concerned that our expression vector might be more potent than the endogenous promoter, running the risk of over-expression. When NRP cells were stably transfected with an HA-tagged, constitutively expressed FLIP short gene, these indicators of apoptosis were absent (Figures 2, 3, 4). Further, NRP clones expressing very low levels of FLIP short failed to show any change in these indicators, while those expressing moderate levels showed an intermediate phenotype, suggesting the dose of FLIP expression is crucial in determining its effectiveness in blocking cell death in normal prostate cells.

If FLIP short antagonizes TGFß-induced apoptosis by inhibiting caspase-8, both proximal and distal caspase mediated cleavage events should be attenuated. Proximally, we sought to measure caspase-8 activation. In TGFß-treated sensitive human cells, human caspase-

08 antibody reveals a very small increase in active fragments and enzymatic assays reveal a small increase in caspase-8 activity (Wallace et al., 1995). Unfortunately, neither this human antibody nor other antibodies tested (DNS) detect the rat caspase-8 active fragments, and we have not been able to identify a suitably sensitive antibody for the rat caspases. Therefore, we used an assay for the cleavage of the caspase peptide substrates in TGFß treated NRP cells. We found that while we could easily detect an increase in caspase-8 activity at late (36-48 hour) timepoints, we could not detect activation of either caspase-8 or -9 at 6, 12, or 18 hours after TGFß addition. Additionally, the later increases in caspase-8 and -9 activities were inhibited when we include an inhibitor of caspase-3, which is highly induced in the lysates and cross-cleaves the IETD (caspase-8) and LEHD (caspase-9) substrates (DNS), suggesting that the both the fold-increase in caspase-8 and the overall amount of active enzyme in TGFß treated NRP cells is small relative to caspase-3. We did see significant increases in the cleavage of caspase-3 and the caspase-3 substrate and apoptosis marker PARP, as well as the caspase-3 peptide substrate (Figure 1). However, when we examine caspase activation in TGFß treated FLIP short expressing clones, we find little or no increase in caspase-3 activity, and that neither caspase-3 itself nor PARP are cleaved in the medium and high expressing clones (Figures 3, 4, and DNS), indicating that these clones are not undergoing the biochemical changes that normally accompany apoptosis in NRP cells.

Since the apoptosis in NRP cells is inhibited by FLIP, and FLIP is thought to principally inhibit the apical caspases, TGFß may be inducing apoptosis by inducing the expression of one of the extracellular death ligands in prostate cells, and DR ECD fusion proteins should block the TGFß-induced apoptosis. To test if FasL is involved in TGFß induced NRP apoptosis, we measured cell death in the presence of rFasFc, a chimeric protein which blocks the interaction

between FasL and Fas. While FasL did induce apoptosis in NRP cells, rFasFc protein failed to block TGFß-induced NRP cell death (Figure 5). TRAIL is thought to be a potent inducer of cell death for prostate cells (Voelkel-Johnson et al., 2002) and the TRAIL receptors are found in both normal prostate (Nesterov et al., 2002)(Vindrieux et al., 2002) as well as a variety of prostate cancer cell lines (Munshi et al., 2001)(Sridhar et al., 2001). Blocking of DR5 has rescued TRAIL-induced prostate apoptosis in normal human prostate cells (Nesterov et al., 2002), but while TRAIL did induce apoptosis in the NRP cells, blocking experiments with the two TRAIL receptor-Fc fusion proteins individually or in combination failed to demonstrate inhibition of the TGFß-induced cell death (Figure 6). It is possible that the human TRAIL receptor is sufficiently different from the rat protein so that the human TRAIL R-Fc fusion proteins that we employed would fail to block rat TRAIL signaling, or one of the other DR ligands (TNF or Tweak) is induced by TGFß, though there is little evidence that they are important in prostate cell death, and so it is unlikely that TGFß is inducing apoptosis in these NRP cells by inducing an extracellular ligand directed apoptosis pathway inhibitable by c-FLIP.

FLIP may inhibit caspase-8 that is not associated with the extracellular death ligand signaling. Insulin and IGF-1 protect against TGFß-induced apoptosis, while EGF does not (Figure 7 and (Song et al., 2003)). IGF-1 inhibits the activation of smad-3, and insulin maintains the intracellular level of FLIP even in the presence of TGFß (Figure 7). Insulin and IGF-1 increase phosphorylation of AKT, which both directly inhibits the activity of Smad-3 (Remy et al., 2004)and Bad (Wanke et al., 2004) and may up-regulate FLIP (Figure 7). Phospo-AKT, and not EGF stimulated phospho-ERK, is associated with increased proliferative index in prostate tumors (Ghosh et al., 2005), suggesting the resistance to apoptosis seen in NRP cells (Figure 7) is reflective of human tumor biology. TGFß-induced apoptosis in gastric carcinoma is FasL

independent and activates Bid cleavage via caspase-8 ((Kim et al., 2004)). It is possible this caspase-8 activity that FLIP is inhibiting in NRP cells.

Materials and Methods

Reagents and Antibodies

Caspase substrates (Biomol), mFasL (UBI), skmTRAIL, DR4-Fc and DR5-Fc (Alexis Biochemicals), TGFß1 (R&D systems), anti-actin (AC-10, Sigma), anti-PARP (C2.10, Enzyme Systems) were purchased from the indicated suppliers. Antibody against the rat $FLIP_L$ C-terminal peptide QVEESLDEDEKEC was prepared in rabbits and purified on a peptide column.

Cell culture and apoptosis

Passage 27 NRP-152 cells were obtained from D. Danielpour (Case Western Reserve University) and maintained as described (Danielpour et al., 1994). Briefly, the cells were cultured in GM2 (Dulbecco's modified Eagle's medium/F12 medium containing 5% fetal bovine serum, 20 ng/ml epidermal growth factor (BD Biosciences), 0.1 mM dexamethasone (Sigma), 10 ng/ml cholera toxin (Sigma), and 350 nM insulin (Biosource)) and passaged before reaching confluence. NRP cells were discarded after 15 passages, except the FLIP expressing clones, which range from 20 to 25 passages after selection. Apoptosis assays were performed in differentiation media (Dulbecco's modified Eagle's medium/F12 containing 1% calf serum, 15 mM HEPES, and 0.1 mM dexamethasone) using 10 ng/ml TGF-ß1 or vehicle (4 mM HCl, 1 mg/ml bovine serum albumin). Rat FLIP short cDNA was cloned and a HA tag added onto the c-terminus, then cloned into the KpnI and ApaI sites of pcDNA3.1 (Invitrogen) to create pratFLIPsHA, and transfected with Lipofectamine (Life Technologies, Inc.) and selected using G418 (GibcoBRL) at 200 ng/ml in GM2. After TGFß treatment, NRP cells that adhere to tissue culture plates through two PBS

washes exclude trypan blue stain, the nuclei appear non-apoptotic by DAPI staining, and show no caspase activation by western blot. In contrast, the detached cells are uniformly apoptotic when recovered from the GM3 media and PBS washes. These detachable cells are apoptotic by DNA laddering, caspase activation by Western blot analysis, and DAPI nuclear staining (DNS and (Chipuk et al., 2001)). Quantification of NRP detachable cells and adherent cells released by trypsin treatment after the PBS washes using a Coulter counter is therefore an accurate measure of apoptosis for TGFß killing of NRP cells. The percent apoptotic cells (% apoptosis) a measure of the detachable cells in the TGFß treated dishes relative to the untreated control dishes.

DNA isolation and labeling

DNA was extracted from a pellet of both attached and floating NRP cells by extraction in 7M guanidine hydrochloride and subsequent isolation of fragmented DNA using the Wizard system (Promega) as described previously (Nastiuk, 2003). DNA fragments were end-labeled with ^{32}P-ddATP and terminal deoxynucleotide transferase (TdT), according to Tilly and Hsueh (Tilly & Hsueh, 1993). The labeled DNA was separated on a 2% agarose gel, dried, and autoradiographed.

Caspase activity assays

NRP-152 cells were treated with TGF-ß1 or vehicle for 36 h. Both adherent and floating cells were harvested and washed with PBS, and counted. The cells were extracted in a buffer containing 20 mM EDTA, 5 mM Tris, pH 8.0, and 0.5% Triton X-100 to isolate caspase-containing cytoplasm. Extract from 400,000 cells was resuspended in a buffer containing 0.1% CHAPS, 50 mM DTT, 50 mM HEPES, pH 7.4, 100 mM NaCl, 1 mM EDTA and 10% glycerol, as well as 50 µM DEVD-pNA (caspase-3 substrate), 100 nM IETD-CHO (caspase-8 inhibitor) and 5 nM YVAD-CHO (caspase-1 inhibitor). The assays were incubated at 37°C and production

of pNA was monitored at 405 nm for three hours. Activity was determined from the slope of the curve in the linear range for each sample, and each sample was assayed in triplicate.

Production and isolation of rat Fas-Fc

Full-length rat Fas was cloned by PCR into pBluescript and the ECD excised and cloned into pB-CD5Lneg1 (Zettlmeissl et al., 1990) containing the CD5 leader sequence and the human Fc domain. This construct or the CD5L-Fc only fragment were excised and inserted into pMT2T to create pMT2T-ratFasECD-Fc. 293 cells were transfected with the rFas-Fc construct, or the CD5L-Fc only fragment , and the protein was isolated from the media using a proteinA column (BioRad).

Cell growth assays

In some cases cell growth were assessed by WST-1 (Boehringer) conversion to formazan. NRP or Jurkat cells were plated in 96-well plates at 2,000 cells/well in RPMI/10% FBS or 10,000 cells/well in GM3, respectively. Fc-receptor was added at the indicated concentration at plating. After 3 hours, FasL, TRAIL, TGFß, or vehicle were added. After an additional 18 h (Jurkat) or 72 h (NRP), Wst-1 was added plates incubated at 37°C and absorbance at 450 nm (less background absorbance at 600 nM) was measured in a microplate reader. Conversion rates were derived from the slope of the curve in the linear range for each sample.

Acknowledgements

We would like to thank D. Danielpour for providing the NRP-152 cell line. This research was supported by grant PC030937 from the USAMRMC Prostate Cancer Research Program.

References

Abedini, M.R., Qiu, Q., Yan, X. & Tsang, B.K. (2004). *Oncogene*, **23,** 6997-7004.

Bin, L., Li, X., Xu, L.G. & Shu, H.B. (2002). *FEBS Letters*, **510,** 37-40.

Brodin, G., ten Dijke, P., Funa, K., Heldin, C.H. & Landstrom, M. (1999). *Cancer Res*, **59,** 2731-8.

Chipuk, J.E., Bhat, M., Hsing, A.Y., Ma, J. & Danielpour, D. (2001). *J Biol Chem*, **276,** 26614-21.

Colombel, M.C. & Buttyan, R. (1995). *Methods Cell Biol.*, **46,** 369-85.

Coyle, B., Freathy, C., Gant, T.W., Roberts, R.A. & Cain, K. (2003). *J Biol Chem*, **278,** 5920-8.

Danielpour, D. (1999). *J Cell Sci*, **112 (Pt 2),** 169-79.

Danielpour, D., Kadomatsu, K., Anzano, M.A., Smith, J.M. & Sporn, M.B. (1994). *Cancer Res*, **54,** 3413-21.

Ghosh, P.M., Malik, S.N., Bedolla, R.G., Wang, Y., Mikhailova, M., Prihoda, T.J., Troyer, D.A. & Kreisberg, J.I. (2005). *Endocr Relat Cancer*, **12,** 119-34.

Goltsev, Y.V., Kovalenko, A.V., Arnold, E., Varfolomeev, E.E., Brodianskii, V.M. & Wallach, D. (1997). *J Biol Chem*, **272,** 19641-4.

Hedlund, T.E., Duke, R.C., Schleicher, M.S. & Miller, G.J. (1998). *Prostate*, **36,** 92-101.

Hedlund, T.E., Meech, S.J., Srikanth, S., Kraft, A.S., Miller, G.J., Schaack, J.B. & Duke, R.C. (1999). *Cell Death Diff*, **6,** 175-182.

Hsing, A.Y., Kadomatsu, K., Bonham, M.J. & Danielpour, D. (1996). *Cancer Res*, **56,** 5146-9.

Inohara, N., Koseki, T., Hu, Y., Chen, S. & Nunez, G. (1997). *Proc Natl Acad Sci U S A*, **94,** 10717-22.

Isaacs, J.T. (1984). *Prostate*, **5,** 545-57.

Kelly, M.M., Hoel, B.D. & Voelkel-Johnson, C. (2002). *Cancer Biol Ther*, **1,** 520-7.

Kim, I.Y., Ahn, H.J., Zelner, D.J., Park, L., Sensibar, J.A. & Lee, C. (1996). *Mol Endocrinol*, **10,** 107-15.

Kim, S.G., Jong, H.S., Kim, T.Y., Lee, J.W., Kim, N.K., Hong, S.H. & Bang, Y.J. (2004). *Mol Biol Cell*, **15,** 420-34.

Kundu, S.D., Kim, I.Y., Yang, T., Doglio, L., Lang, S., Zhang, X., Buttyan, R., Kim, S.J., Chang, J., Cai, X., Wang, Z. & Lee, C. (2000). *Prostate*, **43,** 118-24.

Kyprianou, N. & Isaacs, J.T. (1989). *Mol. Endocrinol.*, **3,** 1515-1522.

Leverkus, M., Sprick, M.R., Wachter, T., Denk, A., Brocker, E.B., Walczak, H. & Neumann, M. (2003). *J Invest Dermatol*, **121,** 149-55.

MacFarlane, M. (2003). *Toxicol Lett*, **139,** 89-97.

Martikainen, P., Kyprianou, N. & Isaacs, J.T. (1990). *Endocrinology*, **127,** 2963-8.

Munshi, A., Pappas, G., Honda, T., McDonnell, T.J., Younes, A., Li, Y. & Meyn, R.E. (2001). *Oncogene*, **20,** 3757-65.

Nagata, S. (1997). *Cell*, **88,** 355-365.

Nagata, S. & Golstein, P. (1995). *Science*, **267,** 1449-1456.

Nastiuk, K.L., Kim, J.W., Mann, M., Krolewski, J.J. (2003). *Journal of Cellular Physiology*, **196,** 386-393.

Nesterov, A., Ivashchenko, Y. & Kraft, A.S. (2002). *Oncogene*, **21,** 1135-40.

Peter, M.E. & Krammer, P.H. (2003). *Cell Death Differ*, **10,** 26-35.

Remy, I., Montmarquette, A. & Michnick, S.W. (2004). *Nat Cell Biol*, **6,** 358-65.

Rippo, M.R., Moretti, S., Vescovi, S., Tomasetti, M., Orecchia, S., Amici, G., Catalano, A. & Procopio, A. (2004). *Oncogene*, **23,** 7753-60.

Rokhlin, O.W., Bishop, G.A., Hostager, B.S., Waldschmidt, T.J., Sidorenko, S.P., Pavloff, N., Kiefer, M.C., Umansky, S.R., Glover, R.A. & Cohen, M.B. (1997). *Cancer Res.*, **57,** 1758-1768.

Rokhlin, O.W., Guseva, N.V., Tagiyev, A.F., Glover, R.A. & Cohen, M.B. (2002). *Prostate*, **52,** 1-11.

Sasaki, Y., Ahmed, H., Takeuchi, T., Moriyama, N. & Kawabe, K. (1998). *Br. J. Urol.*, **81,** 852-855.

Shu, H.B., Halpin, D.R. & Goeddel, D.V. (1997). *Immunity*, **6,** 751-63.

Siegmund, D., Hadwiger, P., Pfizenmaier, K., Vornlocher, H.P. & Wajant, H. (2002). *Mol Med*, **8,** 725-32.

Song, K., Cornelius, S.C., Reiss, M. & Danielpour, D. (2003). *J Biol Chem*, **278,** 38342-51.

Sridhar, S., Ali, A.A., Liang, Y., El Etreby, M.F., Lewis, R.W. & Kumar, M.V. (2001). *Cancer Res*, **61,** 7179-83.

Tang, B., de Castro, K., Barnes, H.E., Parks, W.T., Stewart, L., Bottinger, E.P., Danielpour, D. & Wakefield, L.M. (1999). *Cancer Res*, **59,** 4834-42.

Tilly, J.L. & Hsueh, A.J.W. (1993). *J. Cell. Physiol.*, **154,** 519-526.

Vindrieux, D., Devonec, M., Benahmed, M. & Grataroli, R. (2002). *Mol Cell Endocrinol*, **198,** 115-21.

Voelkel-Johnson, C., King, D.L. & Norris, J.S. (2002). *Cancer Gene Therapeutics*, **9,** 164-72.

Wallace, C.S., Withers, G.S., Weiler, I.J., George, J.M., Clayton, D.F. & Greenough, W.T. (1995). *Brain Research.Molecular.Brain Research.*, **32,** 211-220.

Wanke, I., Schwarz, M. & Buchmann, A. (2004). *Toxicology*, **204,** 141-54.

Xerri, L., Devilard, E., Hassoun, J., Mawas, C. & Birg, F. (1997). *Molecular Pathology*, **50,** 87-91.

Yu, R., Mandlekar, S., Ruben, S., Ni, J. & Kong, A.N. (2000). *Cancer Res*, **60,** 2384-9.

Zettlmeissl, G., Gregersen, J.P., Duport, J.M., Mehdi, S., Reiner, G. & Seed, B. (1990). *DNA Cell Biol*, **9,** 347-53.

Zhang, X., Jin, T.G., Yang, H., DeWolf, W.C., Khosravi-Far, R. & Olumi, A.F. (2004). *Cancer Res*, **64,** 7086-91.

Figure Legends

Figure 1 $FLIP_L$ levels are reduced during TGFß1 induced apoptosis of NRP cells. **(a)** Growth of differentiated NRP cells left untreated (solid bars and square symbol line) or treated with 5 ng/ml TGFß1 (striped bars and circle symbol line). Bars indicate adherent cells (left axis) and lines indicate detached (floating) cells (right axis), each normalized as a percentage of the respective untreated control at 0 h. Error bars correspond to the standard error of the mean. **(b)** Fragmentation of chromosomal DNA in TGFß1 treated NRP cells. Autoradiogram of an agarose gel containing TdT end-labeled nuclear DNA derived from NRP cells grown in growth medium (GM2), 3 h after re-plating in differentiation medium (DF), or after further incubation in differentiation medium containing 5 ng/ml TGFß1 for the indicated time (h). **(c)** Caspase-3 activity in TGFß1 treated NRP-152 cells. DEVD-pNA cleavage was measured in cytosolic extracts of differentiated NRP cells treated with 5 ng/ml TGFß1 for the indicated time (h) as described in the Materials and Methods. Values were normalized to untreated, differentiated cells (n=4). Error bars correspond to the standard error of the mean. **(d)** Immunoblot of PARP cleavage. Nuclear extracts from differentiated NRP cells treated with 5 ng/ml TGFß1 for the indicated time (h) (+), or left untreated (-), were probed with an anti-PARP antibody. The positions of the intact (PARP) and the amino-terminal cleavage product (cleaved) are indicated. **(e)** Immunoblot of $FLIP_L$ protein levels. Cytoplasmic extracts from differentiated NRP cells treated with TGFß1 as in **(d)** were immunoblotted with an anti-FLIP antibody. The positions of the full sized protein ($FLIP_L$) and the 43 kD amino-terminal cleavage product (cleaved) are indicated. The lane labeled "Control" corresponds to lysate from 293T cells transfected with a plasmid encoding $FLIP_L$.

Figure 2 Characterization of stable $FLIP_S$ transfectants (set 1). **(a)** TGFß1 induced apoptosis of $FLIP_S$ transfectants. Cultures were shifted to differentiation media, treated with 5 ng/ml TGFß1 and apoptotic (floating) cells enumerated after 72 h and plotted as per Figure 1a (n=4). Bars correspond to the parental NRP cell line (P), a clone transfected with the vector control (V1), and stable $FLIP_S$ transfected clones (numbered) with varying levels of expression (see **(b)**). **(b)** $FLIP_S$ and control transfectants described in **(a)** were grown in GM2 and protein extracts were immunoblotted with the anti-HA (upper panel), anti-FLIP (middle panel) or anti-actin (lower panel) antibodies. **(c)** Fragmentation of chromosomal DNA following TGFß1 treatment of differentiated NRP transfectants. Similar to Figure 1b; clones were treated with 5 ng/ml TGFß1 for 48 h. Lanes labeled as in **(a)** and **(b)**.

Figure 3 Caspase-3 activity of NRP transfectants. Cultures were differentiated, treated with 5 ng/ml TGFß1 and portions harvested at either 36 h to assay for caspase activity **(b-d)** or at 72 h to quantitate apoptosis **(a)**. **(a)** Apoptosis of $FLIP_S$ transfectants and controls (methods and labeling similar to Figure 2a). **(b)** Caspase-3 enzymatic activity of $FLIP_S$ transfectants and controls was determined and plotted as in Figure 1c (n=3). Samples labeled as in **(a)**. **(c)** Caspase-3 cleavage of $FLIP_S$ transfectants and controls. Cytoplasmic extracts from differentiated cultures (labeled as in **(a))** treated with 5 ng/ml TGFß1 for 36 h (+), or left untreated (-), were immunoblotted with an anti-caspase-3 antibody. The positions of the intact (Casp3) and the amino-terminal cleavage product (p17) are indicated. **(d)** PARP cleavage of $FLIP_S$ transfectants and controls. Nuclear extracts of differentiated cultures treated as in **(c)** were immunoblotted with an anti-PARP antibody. The position of the 117 kD intact PARP and the 84

kDa cleavage product (cleaved) are indicated.

Figure 4 Characterization of $FLIP_S$ transfectants (set 2). **(a-b)** TGFß1 induced apoptosis of $FLIP_S$ transfectants. Additional stable $FLIP_S$ transfected NRP cultures were analyzed as in Figure 2a-b. **(c)** Caspase-3 enzymatic activity of $FLIP_S$ transfectants and controls was determined and plotted as in Figure 3b (n=3). **(d)** PARP cleavage of $FLIP_S$ transfectants and controls was determined as in Figure 3d.

Figure 5 Rat Fas-Fc blocks FasL, but not TGFß1, induced cell death. **(a)** Anti-HA immunoblot of 1 µl purified HA tagged Fc (lane 1) and 1 µl Ha tagged rat Fas-Fc (lane 2) proteins. **(b)** Jurkat cell killing by mFasL is blocked by rFas-Fc. Jurkat cells were treated with diluent (solid bars), 200 pg/ml (diagonal striped bars), or 80 pg/ml (checkered bars) mFasL in the presence of diluent or the indicated amounts of Fc or rFas-Fc. After 18 h, Wst-1 conversion to formazan was measured as described in Materials and Methods and normalized to untreated control Jurkat cells (n=4). Error bars correspond to the standard error of the mean. **(c)** NRP killing by mFasL is blocked by rFas-Fc, but killing by TGFß1 is not. NRP cells were differentiated and then treated with diluent (solid bars), 1 ng/ml (diagonal striped bars) or 5 ng/ml (checkered bars) TGFß1, or 2 ng/ml mFasL (horizontal striped bars) in the presence of diluent or the indicated amounts of Fc or Fas-Fc. After 72 h, Wst-1 conversion to formazan was measured and plotted as in **(b)** (n=4). **(d)** NRP cell killing by TGFß1 is not blocked by high doses of rFas-Fc. NRP cells were differentiated and then either treated with 1 ng/ml TGFß1 or left untreated, in the presence of diluent (none) or the indicated amounts of Fc or Fas-Fc. After 72 h apoptotic (floating) cells were counted and the data plotted as in Figure 1a (n=3).

Figure 6 TRAIL R-Fc blocks FasL, not TGFß, induced cell death. **(a)** Jurkat cell killing by mFasL is blocked by DR4-Fc. Jurkat cells were pre-treated with diluent (solid bars), or 250 ng/ml DR4-Fc (diagonal striped bars) for 3 h, followed by human TRAIL at the indicated concentrations. After 18 h, Wst-1 conversion was measured and plotted as in Figure 5b (n=4). **(b)** Jurkat cell killing by mFasL is blocked by DR5-Fc. Similar to **(a)**, except DR5-Fc was used. **(c)** NRP cells are killed by mTRAIL. NRP cells were treated with the indicated concentration of mouse TRAIL. After 72 h, Wst-1 conversion was measured as in Figure 5b (n=4). **(d)** NRP cell killing by TGFß1 is not blocked by DR4-Fc. NRP cells were pre-treated for 3 h with diluent (solid bars), or 250 ng/ml DR4-Fc (diagonal striped bars) and then treated with the indicated concentration of TGFß1. After 72 h, Wst-1 conversion was measured as in Figure 5b (n=4). **(e)** NRP cell killing by TGFß1 is not blocked by DR5-Fc. Similar to **(d)**, except DR5-Fc was used. **(f)** NRP cell killing by TGFß1 is not blocked by the combination of DR4-Fc and DR5-Fc. Similar to **(d)**, except that a combination of DR4-Fc and DR5-Fc (each at 250 ng/ml) was used.

Figure 7 Insulin increases $FLIP_L$ levels in differentiating NRP-152 cells and blocks apoptosis. **(a)** Insulin blocks TGFß1 induced apoptosis. NRP cells were differentiated for 6 h in the presence of diluent (none), EGF or insulin (at the concentrations used in GM2) and then treated with 5 ng/ml TGFß1 (striped bars) or diluent (solid bars). After 72 h apoptotic (floating) cells were counted and the data plotted as in Figure 1a (n=3). **(b)** EGF and insulin differentially induce $FLIP_L$ expression. NRP cells were differentiated for 6 h in either the absence or presence of insulin or EGF and appropriate extracts were immunoblotted for $FLIP_L$, intact PARP and actin. Representative sample of 3 separate experiments. **(c-d)** Effects of EGF and insulin on

$FLIP_L$ expression and PARP cleavage. NRP cells were differentiated for 6 h in either the absence or presence of insulin or EGF and then either left untreated or treated with 5 ng/ml TGFß1 for 24 or 48 h, all as indicated. Appropriate extracts were immunoblotted as in **(b)**. Representative samples of three separate experiments.

Figure 1

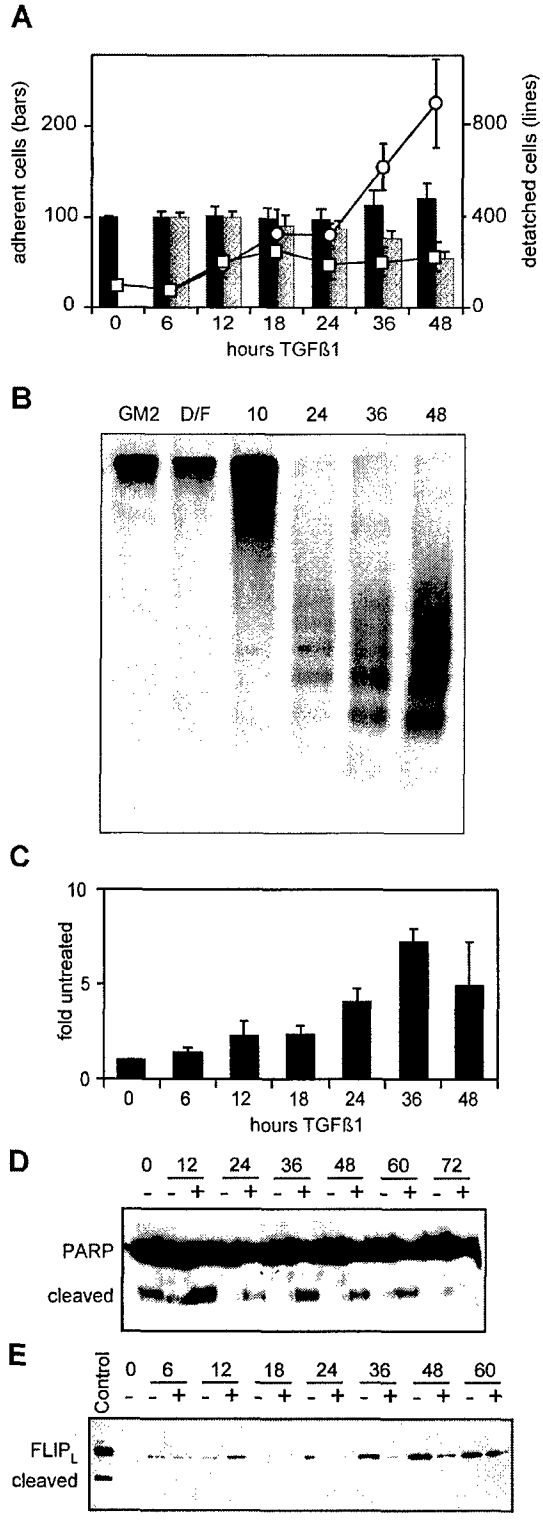
A
adherent cells (bars)
detatched cells (lines)
200
100
0
800
400
0
0 6 12 18 24 36 48
hours TGFß1
B
GM2 D/F 10 24 36 48
C
fold untreated
10
5
0
0 6 12 18 24 36 48
hours TGFß1
D
0 12 24 36 48 60 72
- - + - + - + - + - + - +
PARP
cleaved
E
Control
0 6 12 18 24 36 48 60
- - + - + - + - + - + - + - +
FLIP$_L$
cleaved

Figure 2

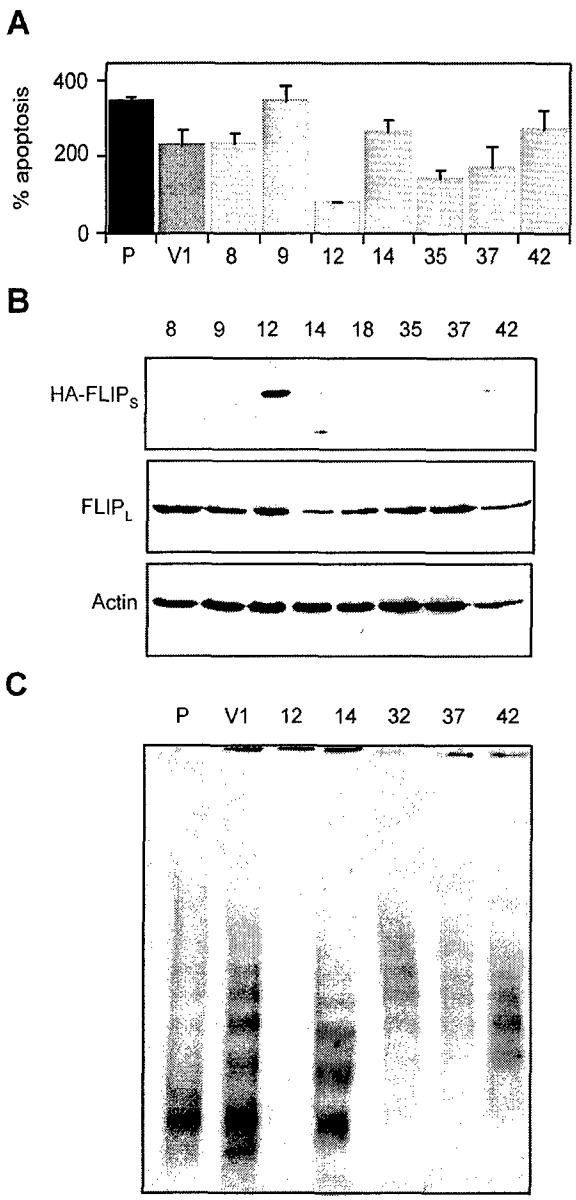
A
% apoptosis
400
200
0
P
V1
8
9
12
14
35
37
42
B
8
9
12
14
18
35
37
42
HA-FLIP$_S$
FLIP$_L$
Actin
C
P
V1
12
14
32
37
42

Figure 3

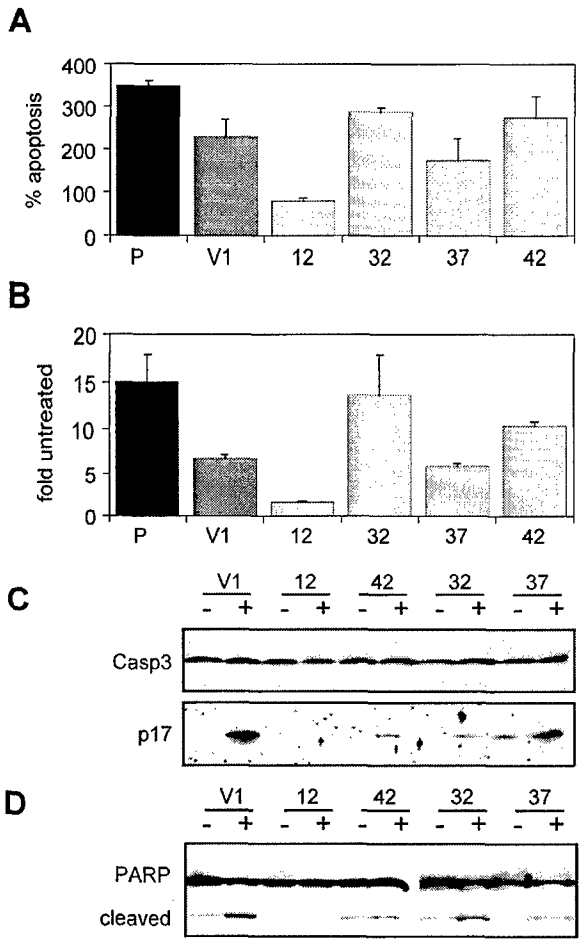
A
400
300
200
100
0
% apoptosis
P
V1
12
32
37
42
B
20
15
10
5
0
fold untreated
P
V1
12
32
37
42
C
V1
12
42
32
37
- + - + - + - + - +
Casp3
p17
D
V1
12
42
32
37
- + - + - + - + - +
PARP
cleaved

Figure 4

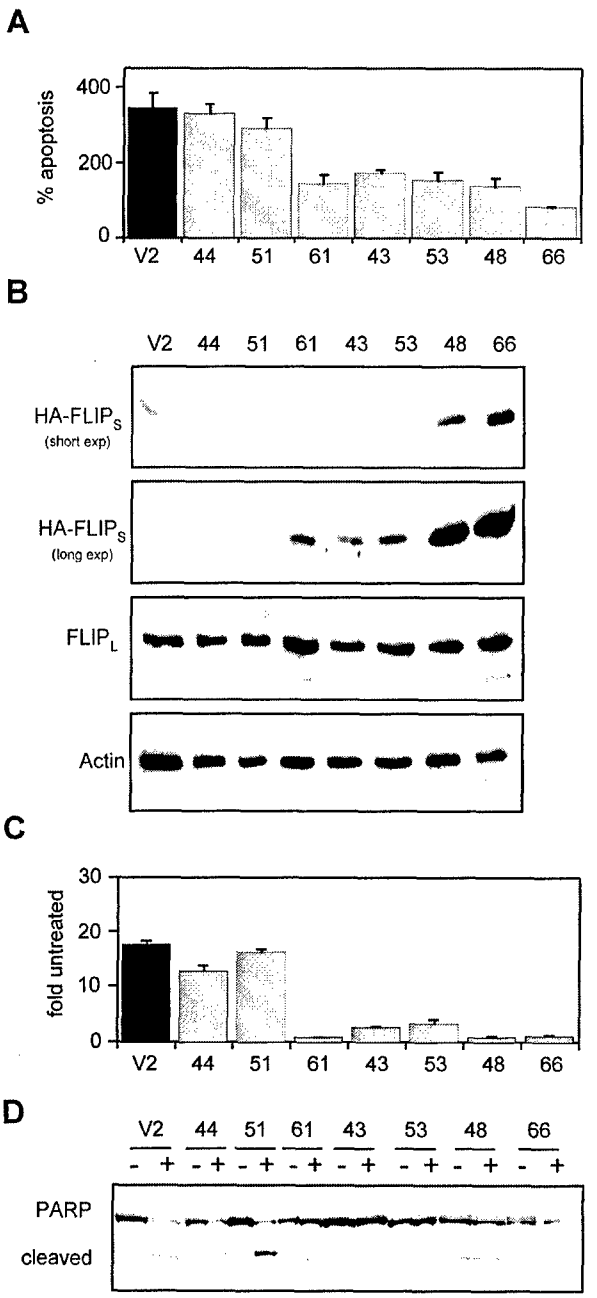
A
% apoptosis
400
200
0
V2 44 51 61 43 53 48 66
B
V2 44 51 61 43 53 48 66
HA-FLIP$_S$ (short exp)
HA-FLIP$_S$ (long exp)
FLIP$_L$
Actin
C
fold untreated
30
20
10
0
V2 44 51 61 43 53 48 66
D
V2 44 51 61 43 53 48 66
- + - + - + - + - + - + - + - +
PARP
cleaved

Figure 5

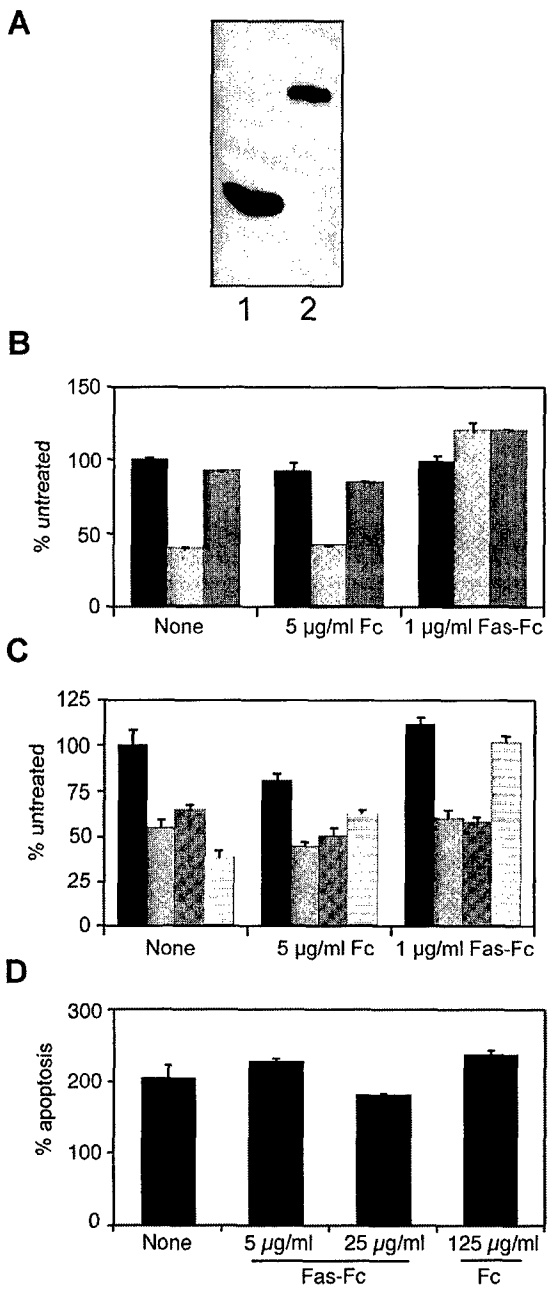
A
1 2
B
% untreated
150
100
50
0
None
5 µg/ml Fc
1 µg/ml Fas-Fc
C
% untreated
125
100
75
50
25
0
None
5 µg/ml Fc
1 µg/ml Fas-Fc
D
% apoptosis
300
200
100
0
None
5 µg/ml
25 µg/ml
125 µg/ml
Fas-Fc
Fc

Figure 6

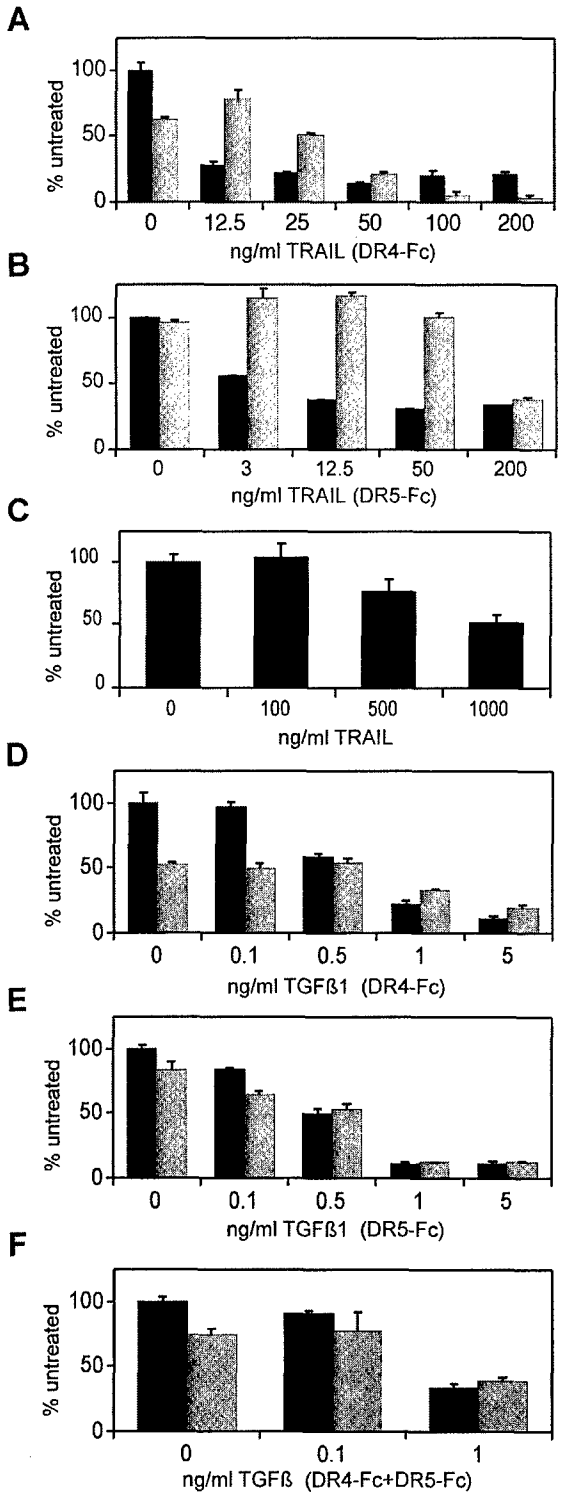
A
% untreated
100
50
0
0
12.5
25
50
100
200
ng/ml TRAIL (DR4-Fc)
B
% untreated
100
50
0
0
3
12.5
50
200
ng/ml TRAIL (DR5-Fc)
C
% untreated
100
50
0
0
100
500
1000
ng/ml TRAIL
D
% untreated
100
50
0
0
0.1
0.5
1
5
ng/ml TGFß1 (DR4-Fc)
E
% untreated
100
50
0
0
0.1
0.5
1
5
ng/ml TGFß1 (DR5-Fc)
F
% untreated
100
50
0
0
0.1
1
ng/ml TGFß (DR4-Fc+DR5-Fc)

Figure 7

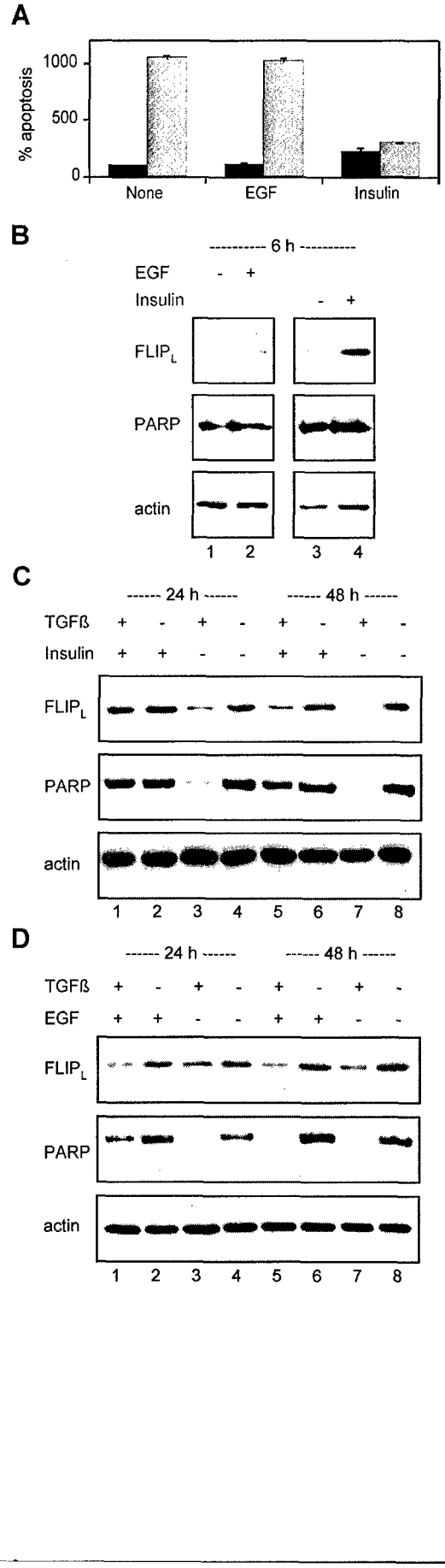
A
% apoptosis
1000
500
0
None
EGF
Insulin
B
6 h
EGF - +
Insulin - +
FLIP$_L$
PARP
actin
1 2 3 4
C
24 h
48 h
TGFß + - + - + - + -
Insulin + + - - + + - -
FLIP$_L$
PARP
actin
1 2 3 4 5 6 7 8
D
24 h
48 h
TGFß + - + - + - + -
EGF + + - - + + - -
FLIP$_L$
PARP
actin
1 2 3 4 5 6 7 8